Journal of Medicinal and Chemical Sciences 6 (2023) 1746-1762

Journal of Medicinal and Chemical Sciences

Journal homepage: http://www.jmchemsci.com/

Original Article

Isolation and Characterization of Hyperoside-Flavanoidal Glycoside from *Rourea Minor* for its Anti-Hyperglycemic Activity Potential: An *In Vitro* Study

Kavya Yedelli, Ramachandran Kumar Pathangi*

Department of Pharmacognosy, SRM College of Pharmacy, SRM Institute of Science and Technology, Kattankulathur, Chennai, Tamil Nadu, India, 603203

ARTICLE INFO

Article history

Receive: 2022-10-13
Received in revised: 2022-11-15
Accepted: 2022-12-15
Manuscript ID: JMCS-2212-1904
Checked for Plagiarism: **Yes**
Language Editor:
Dr. Fatimah Ramezani
Editor who approved publication:
Dr. Behrooz Maleki

DOI:10.26655/JMCHEMSCI.2023.8.4

KEYWORDS

Alpha-amylase
Alpha-glucosidase
Anti-hyperglycemic
Dipeptidyl-peptidase-IV Inhibitor
Hyperoside
Rourea minor

ABSTRACT

To investigate the anti-hyperglycemic activity potential of a hyperoside flavanoidal glycoside isolated from *Rourea minor in vitro*. The study design entails the preparation of *Rourea minor* ethanol stem extract, investigation of its extractive values, total flavonoid content, total phenolic content, high-performance thin layer chromatography, gas chromatography, isolation and characterization of flavanoidal glycosides, cytotoxicity testing, a cell-line study, *in vitro* anti-hyperglycemic activity, and molecular docking analysis using Dipeptidyl-peptidase-IV. The *Rourea minor* ethanol extract has a high percentage yield (25%). Based on the results obtained from the extractive values, *Rourea minor* ethanol extract had the highest (62.6 mg/QA) total flavanoidal content. The phytochemical screening revealed that all of the samples contained phenols, flavonoids, and glycosides confirmed by the thin-layer chromatography results (R_f 0.66). The gas chromatography identified 15 compounds. The isolated compound from *Rourea minor* ethanol extract was separated, and the spectra of these fractions with comparable R_f (0.66) values matched those of the drug, hyperoside ($C_{21}H_{20}O_{12}$). Hyperoside inhibited the enzymes α-amylase, α-glucosidase, and Dipeptidyl-peptidase-IV in vitro while also acting as an anti-hyperglycemic. As a result, using Auto Dock 4.2 software, the presence of hyperoside bound to the Dipeptidyl-peptidase-IV protein was detected at -6.97 kcal/mol. These findings revealed that *Rourea minor* has an anti-hyperglycemic effect.

GRAPHICAL ABSTRACT

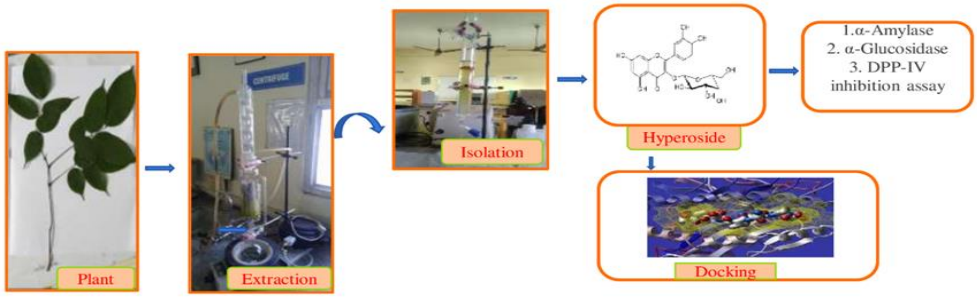

* Corresponding author: Ramachandran Kumar Pathangi
✉ E-mail: Email: pathangikumar70@gmail.com

Introduction

Diabetes symptoms harm a patient's quality of life in terms of their social and psychological well-being as well as their physical health [1, 2]. Species of the genus *Rourea* are known from the Amazon, the Pacific, Africa, and Asia. Some *Rourea* species are poisonous, whereas others are frequently utilized in traditional medicine. Various studies have suggested *Rourea* spices as an anti-hyperglycemic agent. Although they are widely used in ethnomedicine, there are few scientific studies on their chemical ingredients and biological activity [3].

Rourea minor (Gaertn.) Alston (family *Connaraceae)* can be found all across Southeast Asia. They have simple, alternate, spiralling leaves, 12-15 m tall, with petioles of about 2-3.5 cm long and lamina of about 12-30*3-6 cm. The leaves are oblanceolate or obovate-oblong, gradually tapering downwards at the base, abruptly acuminate at the apex, and entire [4]. Two glycosides, rourinoside, and rouremin glucosides are produced by chloroform extraction of the stem of *R. minor* [5]. *R. minor* stems are utilized to detect compounds of bergenin and catechin [6]. A methanol extract from the stem bark of *R. minor* was used to create silver nanoparticles [7]. The roots and twigs are used to make the bitter tonic and uterine tonic, which are used to treat rheumatism, scurvy, diabetes, and pulmonary problems [8]. However, there has not been any *in vitro* anti-hyperglycemic activity study carried out on the young stem of the plant [9] demonstrated that alpha-amylase catalyzes the breakdown of maltotriose and oligosaccharides as starch is hydrolyzed into a combination of smaller oligosaccharides, including maltose. These molecules are converted into glucose by the enzyme alpha-glucosidase, which is then absorbed into the bloodstream [10]. Increased alpha-amylase and alpha-glucosidase activity, which can harm beta cells and reduce insulin synthesis and glucose uptake, are the causes of post-prandial hyperglycemia [8]. The digestion of these enzymes is suppressed at the same time that the metabolism of carbohydrates is slowed down; increasing the time it takes to digest carbohydrates, resulting in lower glucose absorption rates and post-prandial blood glucose levels [11]. Therefore, slowing down carbohydrate digestion by inhibiting alpha-amylase and alpha-glucosidase is a significant target for type 2 diabetes mellitus treatment. The flavonol glycoside hyperoside is present in various plant-based foods [12, 13]. There are several names for quercetin 3-O-D-galactoside. From medicinal herbs, *Hypericum* perforatum [14], *Crataegus davisii* [15], and *Divaricate saposhnikovia* [16] have all been isolated. Hyperoside is linked to anti-inflammatory, anti-diabetic, anti-viral, anti-fungal, and anti-oxidant therapeutic potentials [17]. The present study was aimed at investigating the phytochemical constituents, isolating, and characterizing hyperoside from an ethanol extract of *Rourea minor* stem, investigating the *in vitro* anti-hyperglycemic activity, and docking analysis.

Materials and Methods

Plant material and Authentication

Healthy *R. minor* stems were obtained in Kerala in February. The plant was identified and authenticated by Professor. P. Jayaraman in the Department of Pharmacognosy with the verification voucher number PARC/2020/4367. The remaining stem pieces were dried in the sun, ground into a coarse powder, and used for the study.

Instrument required

The Kohler melting point instrument was used to record the melting points. On a Perkin FTIR spectrophotometer 1650, IR spectra were collected using a KBr disk. H-NMR spectra were acquired at 500 MHz on a JEOL spectrometer with DMSO-d6 as the solvent. A JMS-T 100 LC Mass Spectrometer from JEOL-Accu TOF was used to obtain mass spectra. Silica gel 100-200 mesh (Merck) was used for column chromatography, while silica gel 60PF254 was used for thin-layer chromatography.

Chemicals, assay kits, cell lines, media, and reagents

Reagents and enzymes were purchased from the Hi media laboratory in Chennai, India. Highveld

Biological in South India provided the $HepG_2$ liver cells. Sigma Aldrich in South India provided MTT, which is used in the Eagle's basic fundamental medium (EMEM). Any remaining reagents used in this study were purchased from Sigma.

Determination of the extractive values

Each of the six glass-stoppered dry conical flasks was filled with 4 g of stem powder. One hundred milliliters (100 mL) of various solvents, such as benzene, water, petroleum ether, ethanol, ethyl acetate, and methanol were used to macerate the stem powder for 6 hours with intermittent stirring. After that, the mixture was left for 18 hours before being filtered to a volume of 25 mL. Thereafter, the filtrate was transferred to a flat-bottomed, empty porcelain dish that had been coated with tar. After being evaporated to a dry condition, the residue was dried for six hours at 105 °C, cooled for 30 minutes in a desiccator, and weighed. The percentage (%) yield of the different extracts was estimated using the formula [18].

$$\% \text{ extractive value (w/w)} \frac{(W1 - W2)}{\text{Weight of plant powder taken}} \times 100$$

Preparation of Rourea minor stem extracts

With increasing polarity, different organic solvents such as petroleum ether, ethyl acetate, and ethanol were used to extract the stem powder (60 g). The extraction procedure was carried out three times. Most of the solvent was evaporated under reduced pressure in the rotary evaporator (60 °C). A dark greenish-brown semisolid ethanol extract weighing 10 g was obtained.

HPTLC fingerprinting analysis

By heating 1 gm of the ethanol extract of stems for 10 minutes at 50-550 °C, 1 g of ethanol extract of stems is dissolved in 10 mL of methanol. The extract is filtered before being applied to aluminum monuments (20 × 10 cm) precoated with silica gel 60 F254 from Merck labs. The mobile phase (Chloroform: Ethyl acetate: Formic acid (5:4:1) is saturated using the Whatman filterer paper lining in the Camag twin trough chamber (20 × 10 cm). Using a Linomat V applicator and a Hamilton syringe, a total of 30 µl of ethanol extract solution was applied as an 11.6 mm band. In a twin trough chamber containing the mobile phase, the applied plate was developed. The plate was designed with a 76.5 mm migration distance in mind. It was then scanned with Deuterium and Tungsten lamps at all wavelengths between 254 and 365 nm, and photo documented with Reprostar.

Determination of total flavonoid content

The total flavonoid content (TFC) of the *Rourea minor* ethanol extract (RMEE) was determined using the aluminum chloride colorimetric assay [19]. A high percentage yield of ethanol extract from the subsequent solvent extraction was used in this analysis. A standard solution of the filtrate or a 1 mL aliquot of the RMEE was added to an empty, tarred, flat-bottomed porcelain dish, and evaporated to a dry state. Then, the residue was allowed to dry for six hours at 105 °C before being cooled for 30 minutes in a desiccator and weighed. Using a formula, the percent yield of various extracts was taken into account. Quercetin (20, 40, 60, 80, or 100 µg/mL) was added to a 10 mL volumetric carafe that contained 4 mL of purified water. After another 5 minutes, 0.30 mL of 5% Na_2NO_2 and 0.3 mL of 10% $AlCl_3$ were added to the flask. An aliquot of 5 mL 1 M NaOH was added, and the solution was increased to 10 mL using purified water. After blending the mixture, the absorbance at 510 nm was measured on a UV-visible spectrophotometer (thermos fisher scientific, Chennai). The TFC was expressed as mg of quercetin equivalent (QE). The measurements were made in triplicate.

Estimation of total phenolic content

The Folin-Ciocalteu examiner was used to control the level of total phenolic content (TPC) [19]. Gallic acid (20, 40, 60, 80, or 100 µg/mL) was added to a portion of RMEE concentrate (1 mL) in a 25-mL volumetric carafe containing 9 mL of sterilized water. An aliquot of 1 mL of Folin-Ciocalteu reagent was added to the solution, and then stirred. After 5 minutes, 10 mL of 7% Na_2CO_3 was added to the solution. Then, the volume was increased. After incubation for 90 min at ambient temperature, a UV spectrophotometer was used to

measure the wavelength at 550 nm on a UV-visible spectrophotometer (thermos fisher scientific, Chennai). The amount of total phenolic content was estimated by using gallic acid equivalent (GAE). The measurements were made in triplicate.

Isolation of active constituents

The RMEE was dissolved in methanol before being adsorbed on silica gel with a mesh size of 100–200. It was poured into a column made of silica gel (100-200) that had been manufactured with hexane and the solvent was evaporated. Hexane was used to elute the column, followed by a steady increase in polarity using hexane: ethyl acetate (95:5, 90:10, 80:20, 70:30, 60:40, 50:50, 30:70, and 20:80) and finally with 100% ethyl acetate. To elute the column, a mixture of ethyl acetate and chloroform (90:10, 80:20, 70:30, 60:40, 50:50, 30:70, and 20:80) was used, followed by 100% chloroform. A total of 89 fractions were collected. Thin-layer chromatography was used to monitor the fractions, and similar fractions were found in fractions 72–79 (compound 1). The fractions with similar R_f values were pooled together, and the solvent was evaporated under a lower strain. As a result, fractions were stored at room temperature for an overnight period after being decolored with charcoal (activated) in hot methanol. Analysis of melting point, mass spectra, FT-IR, ^{13}C-NMR, and ^{1}H-NMR spectra of the resultant solid were performed [20].

Gas chromatography

A GC-MS evaluation was carried out on the stem ethanolic extract of *R. minor.* The identification of pharmacologically active natural chemical compositions is done using this method. The experiment was carried out with Agilent (GC-MS QP2022) equipment included an autosampler and a gas chromatograph (GC-MS) apparatus. It functioned under the following circumstances: Column Elite-1 (300.25 mm ID X 1EM df, 100 percent dimethyl polysiloxane), a fused silica capillary column, was used in electron impact mode at 70e V. The carrier gas was helium (99.999 percent) gas, with a continuous flow of 1 mL/min and an injection volume of 1 µL. (split ratio of 10:1). The injector and ion source were kept at 240 °C, respectively. The oven temperature was set to 70 °C (isothermal for 2 minutes), then increased by 10 °C per minute to 300 °C per minute [21], ending with a 9-minute isothermal at 300 °C. The scan range was 40-100 m/z, and the mass spectra were obtained at 70 Ev. The MS start time was 5 minutes, the MS finish time was 35 minutes, and the solvent cut time was 5 minutes. The temperature of the ion source was 200 °C, while the temperature of the interface was 240 °C.

Cell culture maintenance

At 37 °C, all cell cultures were cultured in an environment that was humid and comprised 5% CO_2. Every 2-3 days, $HepG_2$ prison cells were replenished with new ones with development growing media, which consisted of RPMI 1640 standard accompanied by 10% foetal calf serum. After attaining 90% confluence, all cell lines were sub-purified.

Cytotoxicity assay

The cytotoxicity experiments were performed using Mosmann's [22] approach with minor modifications. For the time being, $HepG_2$ liver cells were grown in plates (96 wells) with a capacity of 100 µL at a bulk of 8000 per-well cell count, and the cells were allowed to combine before each well received 100 liters of plant extract at various doses (50 g/mL, 100 g/mL, and 200 g/mL). Instead of 48 hours of heating, the spent media was taken out of the cells and stored at 37 °C by aspiration, and 100 µL of EMEM mixture containing 10% FCS and 0.5 mg/mL MTT was in used and cultured for another 3 hours at 37 °C. After suctioning the media, the MTT valuable stone was destroyed in 10% of DMSO (100 µL) to dissolve in the cells. The formazan jewels were framed. A microplate peruser was used to examine the absorbance at 540 nm Multiscan MS, Lab system). The plant separate's cytotoxic effect was represented as a level of control (medium alone).

$$\% \text{ of inhibition} = \frac{(\text{OD of test} - \text{OD of control})}{\text{OD of test}} \times 100$$

$HepG_2$ Cell' glucose absorption: An experimental procedure

The approach described in Van de Venter's description [23] was used to limit glucose consumption in $HepG_2$ cells. $HepG_2$ cells were extracted with CO_2 and suspended in a new development medium with trypsin (0.25%) in phosphate-supported saline, and grown for three days at 37 degrees Celsius with 5% CO_2 in a 96-well culture plate at a thickness of 4000 cells per well. Two lines without cells were also introduced to function as blanks. On the third day after sowing, the plant (10 µL) ethanol extract with a fixation fraction of 25–100 µg/mL was put into each well without altering the medium. The discarded cultural media aim was replaced after 48 hours with a 25-µL incubation buffer (RPMI mode attenuated with PBS, 0.1 percent BSA, and 8 mm glucose) and incubated for 3 hours at 37 °C. Positive controls included Berberine (0.1 µg/mL) with metformin (0.1 µg/mL) and (18 µg/mL). The negative control consisted of just the incubation buffer and no extract (untreated). To evaluate glucose centralization in the medium, each well received 10 liters of culture broth. After brooding, the culture was relocated to a plate with 96 wells labelled with glucose oxidase reagent (200 µL) to evaluate glucose centralization in the medium. At 37 °C, after 15 minutes of hatching, the measure of glucose used was determined as the contrast between the wells with and without cells. The level of glucose use was determined to correspond to the untreated controls. Using the MTT measurement, cell practicality in the delegate is still up in the air. Through a Multiscan (MS) microtiter plate peruser, the absorbance was determined at 492 nm. The difference between the cells with and without them was used to estimate the glucose concentration. The amount of glucose ingested was assessed in contrast to the untreated controls. Using the MTT measurement, cell practicality in the delegate is still up in the air.

$$\text{Percent of inhibition} = \frac{(\text{OD of test} - \text{OD of control})}{\text{OD of test}} \times 100$$

In vitro anti-hyperglycemic activity testing using alpha-amylase inhibition assay

A slightly modified standard protocol was used to determine the test's α-amylase inhibiting activities by RMEE, and *R. minor* isolated compound (RMIC) [24]. To perform this assay, 100 µL (0.1 mg/mL) of the α-amylase solution was pre-incubated for 15 minutes at 37 °C with different concentrations of the test (10, 20, 40, 80, 160, or 320 µg/mL), reference control (no standard/test), and standard (acarbose) samples. A 100 µL solution of starch was added to initiate the reaction, and it was incubated at 37 °C for 60 minutes. An aliquot of 10 µL HCL (M) and 100 µL iodine reagent was added to the test tubes. The absorption level of the mixture was measured at 565 nm and α-amylase inhibitory activity was measured using the formula [21]:

$$\text{Percentage inhibition} = \frac{(\text{OD of test} - \text{OD of control})}{\text{OD of test}} \times 100$$

The measurements were made in triplicate.

In vitro anti-hyperglycemic activity testing using alpha-glucosidase inhibition assay

The α-glucosidase activity of the test sample, RMEE, and RMIC (hyperoside) was measured. The glucopyranoside-containing p-nitrophenyl (pNPG) substrate solution was made using the enzyme α-glucosidase in a 100 mM phosphate buffer at pH 6.8. An aliquot of 200 µL of α–glucosidase was pre-incubated, and extract fixations of 10, 20, 40, 80, 160, and 320 µg/mL were utilized. After that, the reaction was initiated with 400 µL of 5.0 mM (pNPG) as a substrate that had been liquified in 100 mM of phosphate buffer (pH 6.8). With the addition of 1 mL of 0.1 M Na_2CO_3, the reaction was terminated after 20 minutes at 37 °C. The yellow reaction mixture, 4-nitrophenol, generated by pNPG was measured using a UV-VIS spectrophotometer at 405 nm. Voglibose was used as a positive control, and the inhibitory impact of α-glucosidase was determined with the formula [25]:

$$\text{Percentage inhibition} = \frac{(\text{Abs Control} - \text{Abs Sample}}{\text{Abs Control}} \times 100$$

The measurements were made in triplicate.

Assay to inhibit DPP-IV

The DPP-IV restraint test was done by the technique described by Al-masri with a slight change. Momentarily, 35 µL of RMEE and RMIC

(10, 20, 40, 80, 160, and 320 µg/mL), (di-protein A; 10, 20, 40, 80, 160, and 320 µg/mL) was applied to 15 µL of DPP-IV chemical arrangement (50 U/µL in the barrier of tris) in a separate plate with 96 wells with its wells. The addition of 50 µL of 20 mM NA (Gly-Pro-NA) as the basis for the response was started with the addition of the barrier of tris after 5 minutes of hatching at 37 °C, and the response was further brooded for 30 minutes at 37 °C. Following the incubation period, 25 µL of 25% was added to an acid solution to inhibit the response, and at 410 nm, the absorbance was read. A clear and a test clear were made by substituting 35 µl of a barrier for plant concentrate and 15 liters of support as an alternative to the catalyst. The rate restraint was determined using the accompanying equivalence [26]:

$$\% \text{ of inhibition} = \frac{(\text{OD of test} - \text{OD of control})}{\text{OD of test}} \times 100$$

Docking analysis

The protein data bank of the research collaborative for structural bioinformatics hosted the crystal structure of DPP-IV (PDB ID: 4EWA). The DPP-IV structure was cleaned up before the docking simulation by eliminating the water, ligand, and other unimportant small molecules; adding hydrogen atoms and charges; and fixing residues. The PubChem database mol2 formats of the tested flavanoidal glycoside (hyperoside) were obtained, and the structures were prepared by reducing energy, eliminating water, adding atomic charge, designating an atomic type, and making all flexible bonds rotatable. Using the Auto Dock 4.2 program, molecular docking simulations were run as well as the docking model of a complex with binding energy for hyperoside. The relationship between the hyperoside and DPP-IV was visualized with pymol software.

Results and Discussion

Extractive values

The extractive values for benzene, ethyl acetate, water, petroleum ether, methanol, and ethanol soluble are all listed in Table 1.

Table 1: The extractive values for *Rourea minor* extraction with various solvents

Extract	Colour	% yield (w/w)
Benzene	Brown	2 **%**
Ethyl acetate	Light yellow	4 **%**
Water	Brown	8 **%**
Petroleum ether	Light yellow-green	12 **%**
Methanol	Yellowish-brown	15 **%**
Ethanol	Dark greenish brown	25 **%**

HPTLC report

The ethanol extract of stems was subjected to HPTLC analysis. At R_f of 0.19, 0.29, 0.32, 0.36, 0.40, 0.43, 0.48, 0.50, 0.53, 0.57, 0.60, 0.62, 0.65, 0.67, and 0.71, stem extract eluted 15 phytoconstituents, the most prominent spots are at R_f 0.19, 0.32, 0.48, 0.50, 0.53, 0.60, 0.65, and 0.71, while others are less prominent under 254 nm. All of the spots are brown-dark green under UV 254 nm, but the spots at R_f 0.47 fluoresced buff green with the standard under UV 365 nm. Blue fluorescence was seen at R_f 0.02, 0.06; dark pinkish blue fluorescence was seen at R_f 0.11, 0.23; pink fluorescence was seen at R_f 0.46; dull red fluorescence was seen at R_f 0.53 and 0.70, and pale-yellow fluorescence was seen at R_f 0.60. Peaks at R_f 0.31, 0.39, and 0.66 were prominent in the stem extract, as indicated in Table 2 and Figure 1.

Table 2: HPTLC Fingerprints of *R. minor* stem ethanol extract

HPTLC effect on ethanol extract from stems			
Peak	Maximum Rf	Area (AU)	Percentage area (%)
1	0.19	302.6	3.903
2	0.29	440.3	5.69
3	0.32	373.4	4.82
4	0.36	462.2	5.97
5	0.40	93.4	1.20
6	0.43	1193	15.43
7	0.48	949.7	12.28
8	0.50	514.9	6.66
9	0.53	1438.6	18.61
10	0.57	361	4.65
11	0.60	575.9	7.45
12	0.62	238.5	3.08
13	0.65	407	5.26
14	0.67	177.5	2.29
15	0.71	214.9	2.77

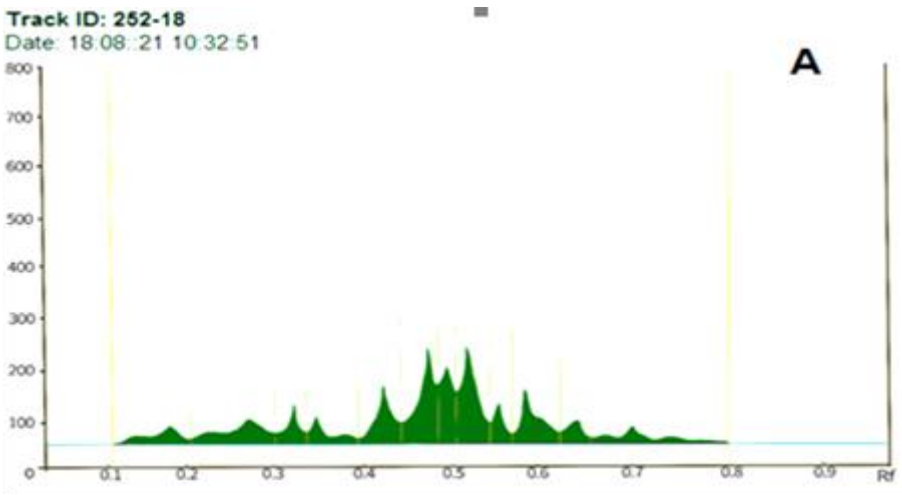

Figure 1: Stem ethanol extract

The total flavonoid and phenolic contents of Rourea minor ethanol extract

The standard calibration equations for total flavonoid content were reported in terms of quercetin equivalent as y = 0.0259x + 0.3285, R^2 = 0.9599 with a mean value of 62.6 mg of quercetin/g of dry extract, as displayed in (Figure 2).

The total phenolic content was presented in terms of gallic acid equivalent y = 0.0213x + 0.1288, R^2 = 0.9476) with a mean value of 43.9 mg of gallic acid/g of dry extract.

Active phytochemicals in Rourea minor ethanol extract

When *Rourea minor* ethanol extract was separated, the spectra of these fractions with comparable R_f (0.66) values matched those of the drug, hyperoside.

Mass spectrum

Some of the active phytochemicals discovered in the ethanol extract of *Rourea minor* include $C_{21}H_{20}O_{12}$, EI-MS m/z: 465.1 [M+H] +, 487.09 [M+ Na] +, as shown in (Figure 3). The compounds were pale yellow solids with a melting point of 232-234 °C.

^{1}H-NMR (DMSO-d_6) ppm

12.62 (1H, s, -OH), 9.69 (1H, s, -OH), 9.12 (1H, s, -OH), 7.64-7.67 (1H, dd, -Ar-H), 7.50- 7.51 (1H, d, -

Ar-H), 6.79- 6.81 (1H, d, -Ar-H), 6.38 – 6.39 (1H, d, -Ar-H), 6.18 – 6.19 (1H, d, Ar-H), 5.35 – 5.37 (1H, d, H-1"), 5.09 -5.10 (1H, d, Glucose-OH), 4.81 -4.83 (1H, d, Glucose-OH), 4.41-4.43 (1H, m, Glucose-OH), 4.38-4.40 (1H, m, Glucose-OH), 3.63 (1H, s, H-4"), 3.52-3.58 (1H, m, H-2"), 3.41 -3.45 (1h, m, H-6"a), and 3.25 -3.37 (2H, m, H-3", H-5", and H-6"b), as displayed in Figure 4.

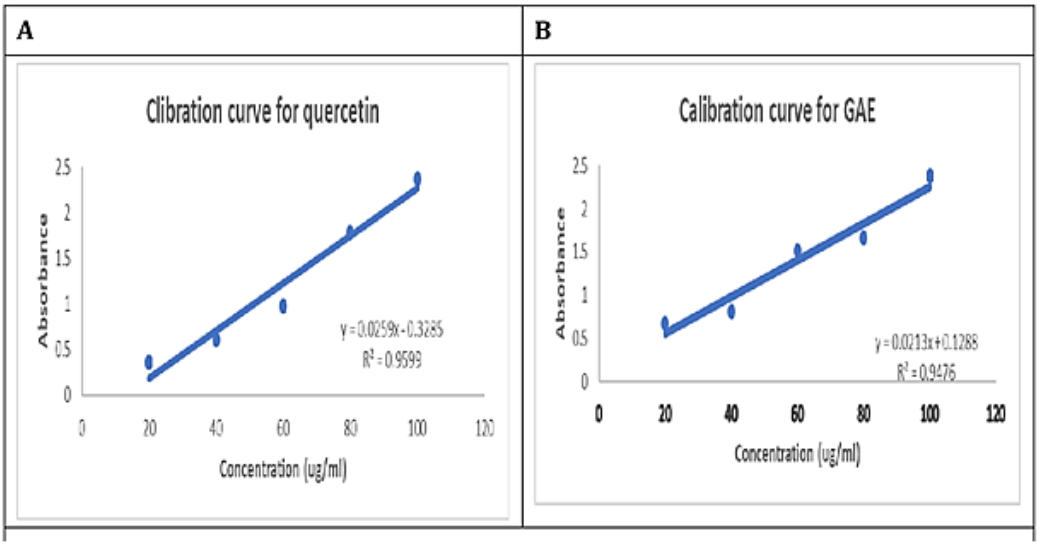

Figure 2: Calibration curves to determine total flavonoids (A) and total phenolic compounds (B)

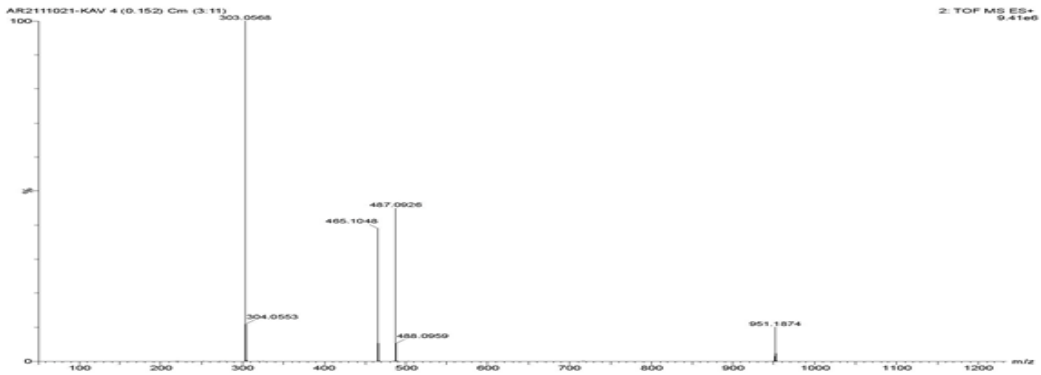

Figure 3: Mass spectrum EI-MS m/z of phytoconstituent

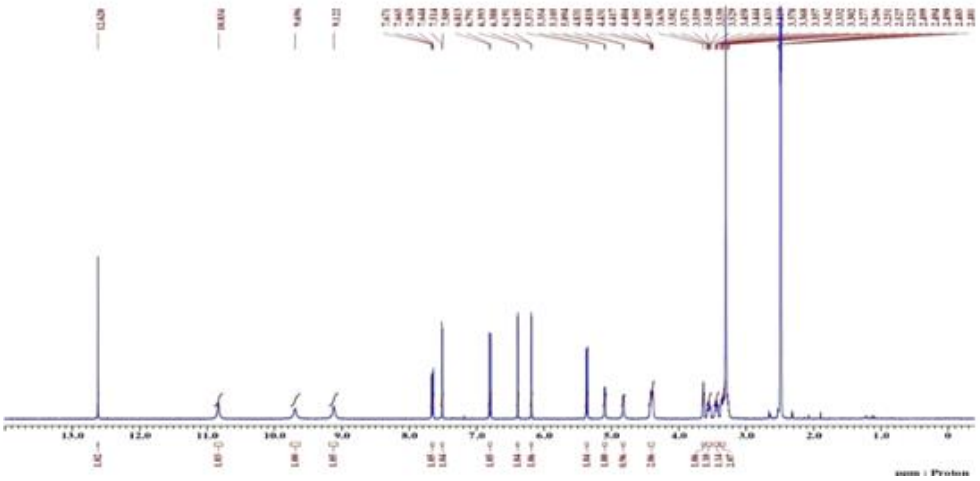

Figure 4: Flavanol glycoside 500 MHz ^{1}H-NMR spectrum. Hyperoside was enzymatically obtained from DMSO-d_6

^{13}C-NMR (DMSO-d_6)

δ 177.49 (C-4), 164.11 (C-7), 161.22 (C-5), 156.29 (C-9), 156.22 (C-2), 148.45 (C-4'), 144.82 (C-3'), 133.47 (C-3), 121.99 (C-6'), 121.09 (C-1'), 115.94 (C-2'), 115.17 (C-5'), 103.92 (C-10), 101.78 (C-1), 98.66 (C-6), 93.48 (C-8), 75.83 (C-5), 73.18 (C-3''), 71.20 (C-2''), 67.92 (C-4''), and 60.14 (C-6''), as depicted in Figure 5.

FT-IR (KBr)

3467, 3320 cm^{-1} (-OH stretching), 2975, 2902 cm^{-1} (-CH stretching), 1656 cm^{-1} (-C = C stretching); 1608 cm^{-1} (-C = O stretching), 1445 cm^{-1} (-CH stretching), and 1364 cm^{-1} (-CH bending), as illustrated in Figure 6.

The spectral pattern was the same as the hyperoside shown in Figure 7.

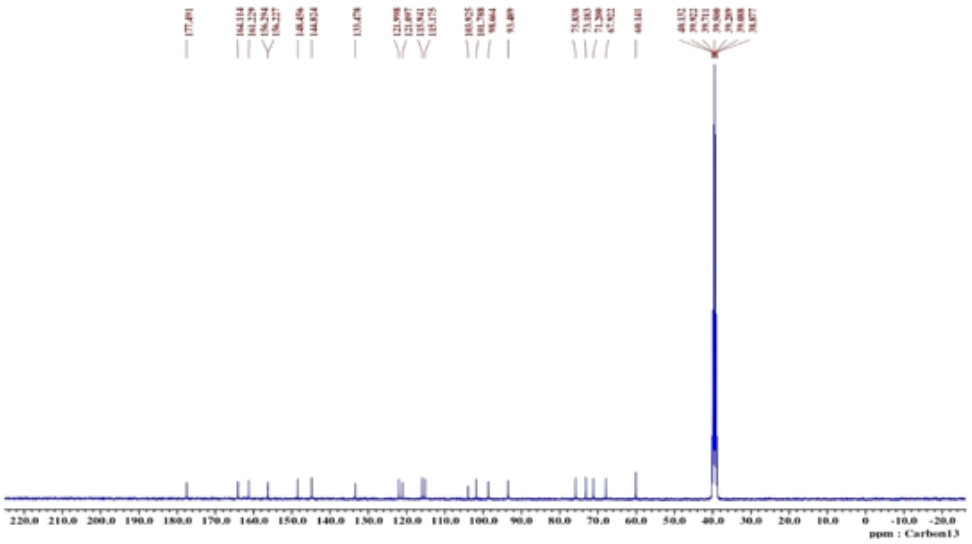

Figure 5: ^{13}C-NMR spectrum of hyperoside

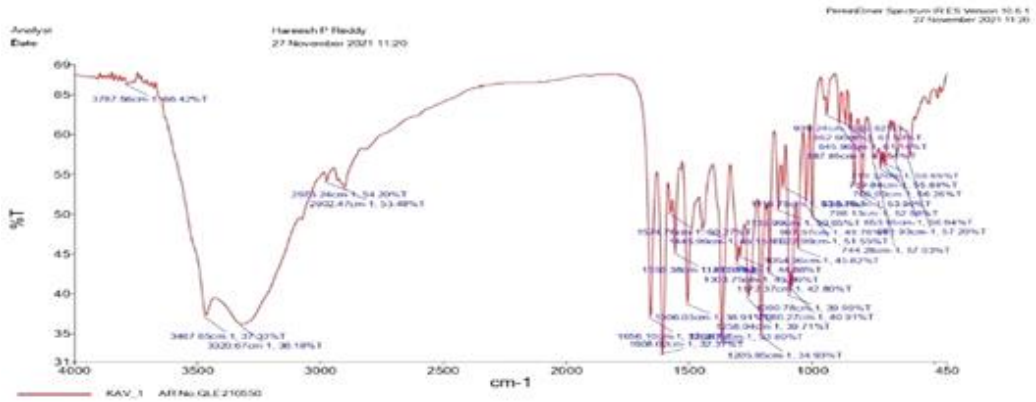

Figure 6: KBr disc on Perkin Elmer FTIR spectrophotometer 1650 for compounds that indicate the presence of functional groups by characteristic absorption of hyperoside

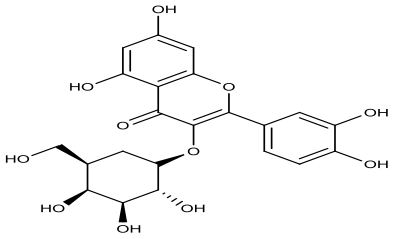

Figure 7: Hyperoside ($C_{21}H_{20}O_{12}$) structure

Gas chromatography

A total of 15 compounds are identified and listed in Figures 8, GC-MS analysis in that major antidiabetic activity reported compounds and higher peak area percentage are 1,5-Anhydrogluitol (56.07%), *n*-Hexadecanoic acid (3.57%), and phytol (2.43%), with a lower peak area percentage of 1,1-diethoxy-3-methyl-Butane (0.31%). 1,5-anhydrous glucitol has been shown to have anti-diabetic activity [27], *n*-hexadecanoic acid has been shown to have anti-inflammatory [28] and anti-diabetic activity [29], and also phytol has been shown to have anti-inflammatory [30] and anti-diabetic activity [31].

By synchronizing the target compounds with hits from the library in the database, the following interpretations were done. Glycidol MS (ESI): m/z: 74, M^+ parent peak calculated for $C_3H_6O_2$; characteristic intense base peak at 44 accounts for the fragment C_2H_4O.

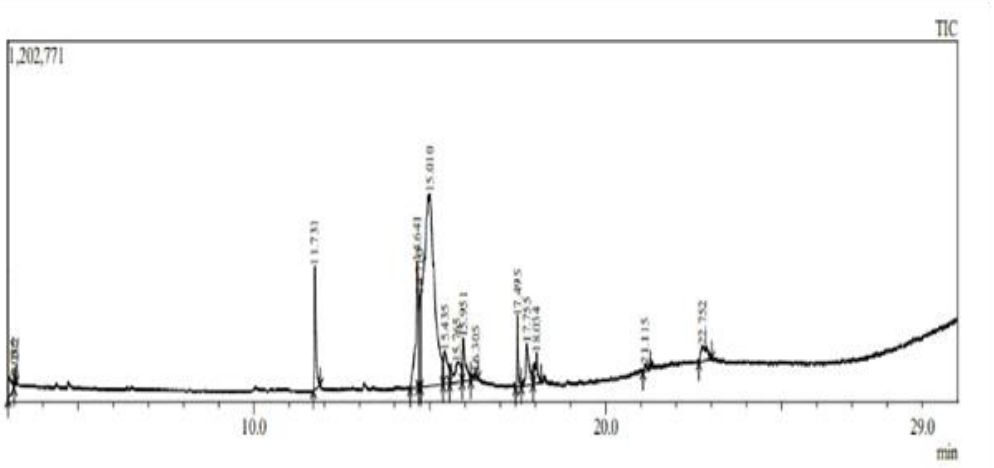

Figure 8: Gas chromatography-mass spectrum of *R. minor* stem ethanol extract

1-Ethoxy-3-methyl-butane MS (ESI): m/z: 115, M+1 parent peak calculated for $C_7H_{16}O + H^+$; characteristic intense base peak at 103 accounts for the fragment $C_6H_{14}O + H^+$. Diethyl Phthalate MS (ESI): m/z: 222.1, parent peak calculated for $C_{12}H_{14}O_4$; characteristic intense base peak at 149.05 accounts for the fragment $C_8H_6O_3$. 2-Hexadecen-1-ol MS (ESI): m/z: 240, parent peak calculated for $C_{12}H_{14}O_4$; characteristic intense base peak at 95 accounts for the fragment C_7H_{12}. 4-ethyl-2-methylhexan-1-ol MS (ESI): m/z: 145, parent peak calculated for $C_9H_{20}O$; characteristic intense base peak at 70.10 accounts for the fragment C_5H_{10}. 1, 5-Anhydroglucitol MS (ESI): m/z: 164, parent peak calculated for $C_6H_{12}O_5$; characteristic intense base peak at 73 accounts for the fragment C_5H_{12}. 2- Deoxy D-Galactose MS (ESI): m/z: 164, parent peak calculated for $C_6H_{12}O_5$; characteristic intense base peak at 43 accounts for the fragment C_3H_8. (R)-2-methyl-4H-pyran-3,4,5-triol MS (ESI): m/z: 145, parent peak calculated for $C_6H_8O_4$; characteristic intense base peak at 85 accounts for the fragment C_5H_6O. Hexadecanoic acid MS (ESI): m/z: 256, parent peak calculated for $C_{16}H_{32}O_2$; characteristic intense base peak at 73 accounts for the fragment C_5H_{12}. 8-methylnonanoic acid MS (ESI): m/z: 256, parent peak calculated for $C_{12}H_{24}O_2$; characteristic intense base peak at 88.05 accounts for the fragment C_6H_{14}. Phytol MS (ESI): m/z: 298, parent peak calculated for $C_{12}H_{24}O_2$; characteristic intense base peak at 71 accounts for the fragment C_5H_{12}. Z, Z-8,10-Hexadecadien-1-ol MS (ESI): m/z: 238, parent peak calculated for $C_{16}H_{30}O$; characteristic intense base peak at 55 accounts for the fragment C_4H_6. 9, 12-Octadecadienoic acid (Z, Z) MS (ESI): m/z: 280, parent peak calculated for $C_{18}H_{32}O_2$; characteristic intense base peak at 67 accounts for the fragment C_5H_{10}. Octadecanoic acid MS (ESI): m/z: 280, parent peak calculated for $C_{18}H_{32}O_2$; characteristic intense base peak at 67 accounts for the fragment C_5H_{10}. Cis-Valerenyl acetate MS (ESI): m/z: 202, parent peak calculated for $C_{17}H_{26}O_2$; characteristic intense base peak at 173 accounts for the fragment $C_{13}H_{18}$.

Cytotoxicity

The MTT assays were performed on the $HepG_2$ liver cell line at various fixations and were used to determine the *in vitro* cytotoxic movement of the *R. minor* ethanol concentrate. The cytotoxicity results showed that *R. minor* concentrate demonstrated toxicity to $HepG_2$ cells in a dose-dependent manner (Figure 9). Cell death was observed at the appropriate test dose (200 µg/mL), as the IC_{50} value (concentration capable of killing 63 percent of cells) was discovered to be 200 µg/mL.

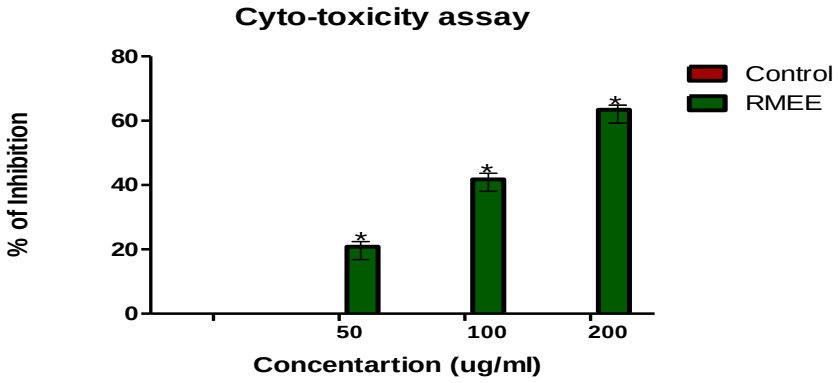

Figure 9: MTT cytotoxicity effect of the ethanol extract of *R. minor* on Cell lines is liver cells that have been genetically modified. The information is shown as a percentage of the control mean ± SD (n = 3). * Specifies a substantial upsurge ($p < 0.05$) when compared with a control group

$HepG_2$ glucose utilization

Figure 10 depicts the consumption of glucose data achieved in $HepG_2$ cells at 25 and 100 µg/mL in the presence of the *R. minor* extricate. The ethanol extract of *R. minor* produced a huge ($p < 0.05$) larger expansion in any focal points of glucose consumption in $HepG_2$ cells as compared with a control group and the Berberine-treated control, except for metformin. Then again, the ethanol extract of *R. minor* (80%) displayed a higher expansion in glucose take-up at 100 µg/mL. It was less than Berberine (80%) but higher than metformin (110%).

The data is provided as a mean ± standard deviation (n = 3). *There was a substantial increase ($p < 0.05$) as compared with the control cell lines.

Alpha-amylase inhibitory effect of Rourea minor ethanol extract

The results demonstrated that the RMEE significantly inhibited alpha-amylase at all test sample concentrations (10, 20, 40, 80, 160, and 320 µg/mL) in a dose-dependent manner. Nonetheless, RMEE was observed to have 98% inhibition at the maximum concentration (320 µg/mL) tested, but this was less than acarbose, which had a 98% inhibition rate (Figure 11A). The percentage of inhibition observed in the RMIC was 93%. However, this was higher than the percentage inhibition recorded for acarbose in Figure 12B. In the alpha-amylase assay, the IC_{50} values of acarbose and RMEE were 5.09 and 25.76, respectively, while 11.74 and 30.9 were recorded for the IC_{50} values of Acarbose and Hyperoside, respectively.

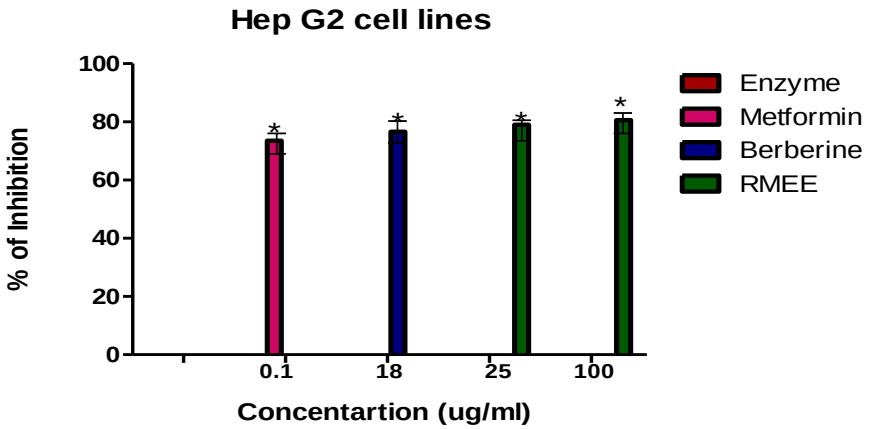

Figure 10: An ethanol extract of *R. minor*'s effect on glucose utilization in Hep G_2 cells was given a 48-hour treatment with varying doses of the presence or absence of a plant extract

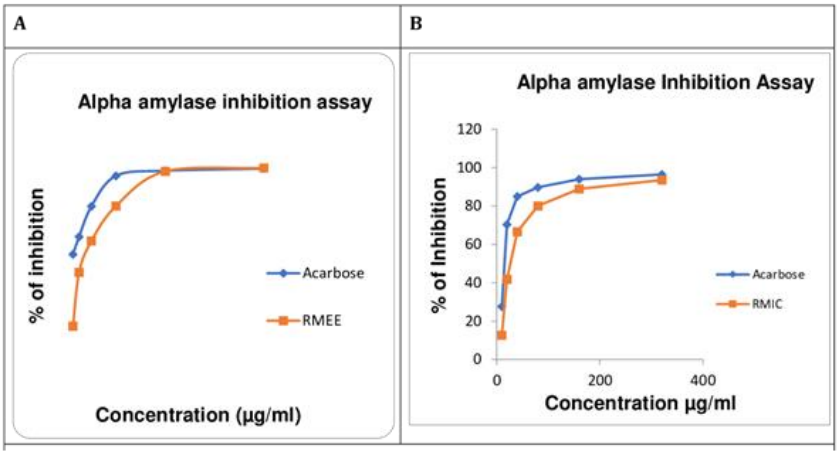

Figure 11: % inhibition of alpha-amylase against RMEE (A) and % inhibition of alpha-amylase against RMIC (B)

Acarbose is a glucosidase inhibitor that prevents complex carbohydrates from being digested and absorbed in the gut [32]. These drugs also increase the release of the gluco-regulatory hormone, glucagon-like peptide-1 into the bloodstream, which could help explain their glucose-lowering effects [33]. According to several scientific findings, phenols and their effects on the inhibitory potentials of α-amylase and α-glucosidase are significantly correlated with flavonoids [34].

Alpha-glucosidase inhibitory activity of Rourea minor ethanol extract

The results revealed that the RMEE significantly inhibited alpha-glucosidase activity at each of the test sample concentrations (10, 20, 40, 80, 160, and 320 µg/mL) in a dose-dependent manner. Nevertheless, 88% inhibition was obtained by the RMEE at the highest concentration (320 µg/mL), which was less than voglibose (91%), as demonstrated in Figure 12A. The RMIC, hyperoside, was observed to have an 83% inhibition rate, but this was higher than voglibose with a 94% inhibition rate as demonstrated in Figure 13B. In the alpha-glucosidase assay, the IC_{50} values of voglibose and RMEE were 34.1 and 66.4%, respectively, while IC_{50} values of 22.7 and 71.9 were respectively recorded for Voglibose and Hyperoside.

Assay for DPP-IV inhibition

The results revealed that the RMEE significantly inhibited DPP-IV at each of the test sample concentrations (10, 20, 40, 80, 160, and 320 µg/mL) in a dose-dependent manner. Nevertheless, 83% inhibition was obtained by the RMEE at the highest concentration (320 µg/mL),

which was less than Diprotin A (93%), as depicted in Figure 13A. The RMIC, hyperoside, was observed to have an 84% inhibition rate, but this was higher than Diprotin A with a 94% inhibition rate, as demonstrated in Figure 14B. In the DPP-IV inhibition assay, the IC_{50} values of Diprotin A and RMEE were 35.1 and 67.4%, respectively, while IC_{50} values of 23.7 and 72.9 were respectively recorded for Diprotin A and Hyperoside.

Among these are alpha-amylase, alpha-glucosidase, and DPP-IV inhibition, in comparison to the positive controls, there was a significant inhibition. A similar observation has been made for flavanoidal glycosides (hyperoside) [35, 36]. The results obtained in this study indicate that the RMEE could be a valuable therapeutic agent for diabetic complications.

Docking with DPP-IV enzyme

Molecular docking was performed to mimic the binding interaction between DPP-IV and hyperoside. Figure 14 and Table 3 show the best docking outcomes. The binding energy of hyperoside to the active pocket of DPP-IV was -6.97 kcal/mol. Seven hydrogen bonds were generated in the hyperoside ARG125, HIS126, SER209, TYR547, TYR585, TYR662, and ASP663 with distances of 3, 3.3, 2.8, 2.7, 3.6, 2.7, and 2.8, respectively.

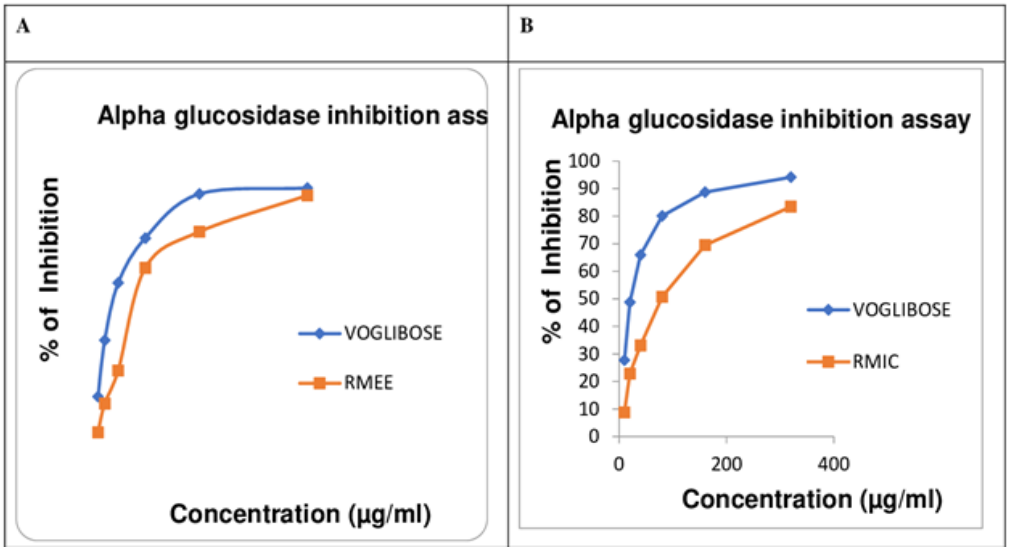

Figure 12: % inhibition of alpha-glucosidase against RMEE (A) and % inhibition of alpha-glucosidase against RMIC (B)

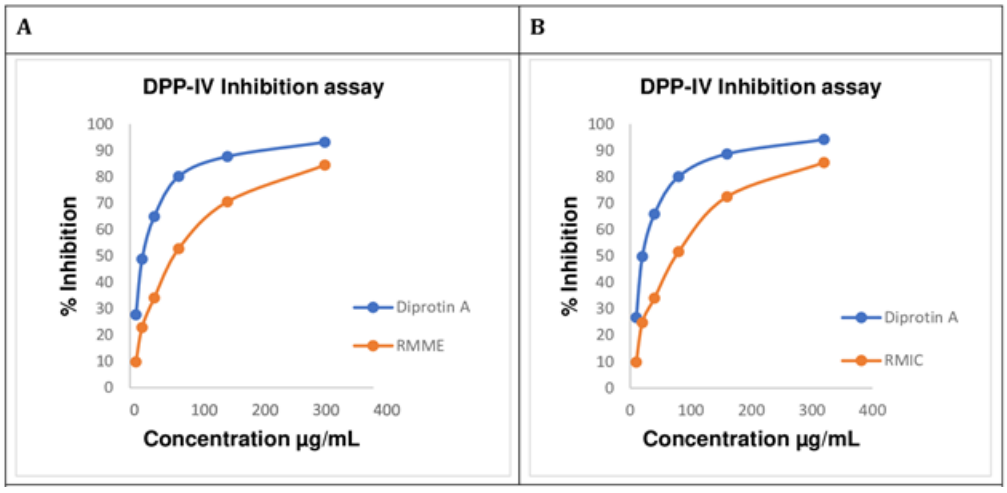

Figure 13: % inhibition of DPP-IV against RMEE (A) and % inhibition of DPP-IV against RMIC (B)

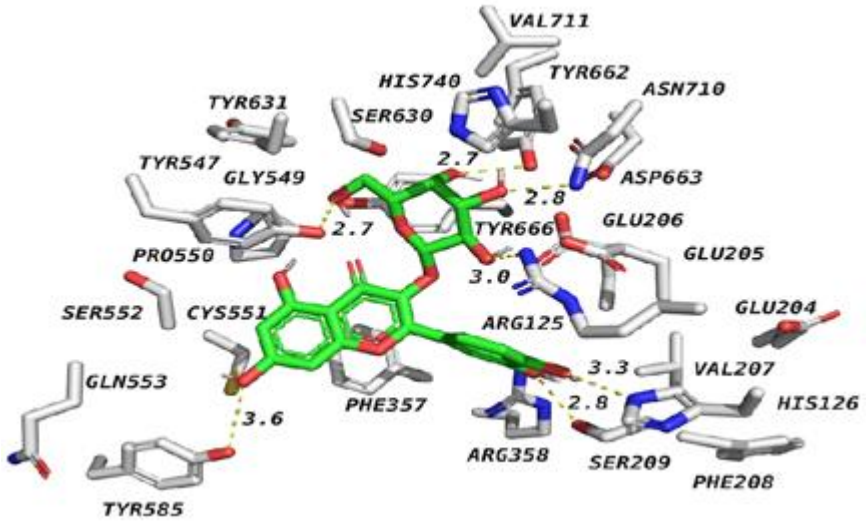

Figure 14: 3D interaction pattern of human dipeptidyl peptidase IV and hyperoside compound

Table 3: Overall docking results of ligand hyperoside

S. No.	Protein	IUPAC	Binding energy (kcal/mol)	Predicted Inhibition Constant	Structure
1	Human Dipeptidyl peptidase IV (PDB ID IRWQ)	(2-(3,4-dihydroxyphenyl)-5,7-dihydroxy-3-[(2S,3R,4S,5R,6R)-3,4,5-trihydroxy-6-(hydroxymethyl) oxan-2-yl] oxychromen-4-one	-6.97	7.78μM	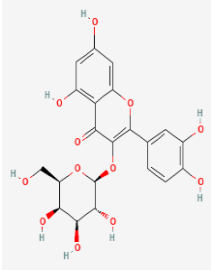

In addition, hyperoside interacted with the hydrophobic interactions of VAL207, PHE208, PHE357, GLY549, PRO550, CYS551, and VAL711, hydrophilic interaction: GLU204, GLU205, GLU206, ARG358, SER552, GLN553, SER630, TYR631, TYR666, ASN710, and HIS740, as well as hydrogen bond interactions: ARG125, HIS126, SER209, TYR547, TYR585, TYR662, and ASP663.

Molecular docking provides an essential tool for drug discovery. Binding energy is the critical parameter to provide for us an idea about the strength and affinity of the interaction between the ligand and receptor. Greater the binding energy, the weaker the interaction is, and vice versa. In this study, hyperoside displayed binding energy against the DPP-IV enzyme, indicating a good interaction. Flavanoidal glycosides such as hyperoside acted as DPP-IV inhibitors, and *in silico* analysis showed that these flavanoidal glycosides bounds to the enzyme with low binding energy (-6.97 kcal/mol).

Conclusion

In the present study, chloroform: methanol fraction was initially used to extract the chemical flavonol glycoside; hyperoside was discovered as a fraction of a crude ethanol extract of *Rourea minor* stem. The findings of this study demonstrate that the ethanol extract of *Rourea minor* stem possesses anti-hyperglycemic properties. *Rourea minor* ethanol extract and isolated compound significantly inhibited the enzyme assays for α-amylase, α-glucosidase, and DPP-IV. Based on the *in-vitro* assay findings and the presence of active components, *in-silico* docking studies of hyperoside were done against the DPP-IV enzyme. The molecular docking analysis revealed that compound hyperoside

showed a good enzyme inhibition. More research is needed to determine the potential pharmacological anti-hyperglycemic effectiveness of the extract.

Acknowledgements

The authors appreciate the help they received from SRM College of Pharmacy and SRM University, Kattankulathur, Chennai.

Funding

This research did not receive any specific any specific grant from funding agencies in the public, commercial, or-for-profit sectors.

Authors' contributions

All author's contributed to data analysis, drafting, and revising of the paper and greed to be responsible for all the aspects of this work.

Conflict of Interest

The author declared that they have no conflict of interest.

ORCID

Kavya Yedelli
https://www.orcid.org/0000-0003-4969-5774
Ramachandran Kumar Pathangi
https://www.orcid.org/0000-0002-2737-0365

References

[1]. Basha S.K., Kumari V.S., In-vitro anti-diabetic activity of *Psidium guajava* leaves extracts, *Asian Pacific Journal of Tropical Disease,* 2012, **2**:S98 [Crossref], [Google Scholar], [Publisher]

[2]. Dewanjee S., Das A.K, Sahu R., Gangopadhyay M., Antidiabetic activity of *Diospyros peregrina* fruit: Effect on hyperglycemia, hyperlipidemia and augmented oxidative stress in experimental type 2 diabetes, *Food and chemical toxicology*, 2009, **47**:2679 [Crossref], [Google Scholar], [Publisher]

[3]. Osman C.P., Zahari Z., Adenan M.I, Zohdi R.M., A review on traditional uses, phytochemistry, and pharmacology of the genus rourea, *Journal of Applied Pharmaceutical Science,* 2019, **9**:125 [Crossref], [Google Scholar], [Publisher]

[4]. Chandra D., Mukherjee. *Rourea minor* (Gaertn.) Alston species. *India bio diversity portal*, 2000 [Publisher]

[5]. He Z.D., Ma C.Y., Tan G.T., Sydara K., Tamez P., Southavong B., Bouamanivong S., Soejarto D.D., Pezzuto J.M., Fong H.H., Zhang H.J., Rourinoside and rouremin, antimalarial constituents from *Rourea minor*. *Phytochemistry,* 2006, **67**:1378 [Crossref], [Google Scholar], [Publisher]

[6]. Ngoc H.N., Löffler S., Nghiem D.T, Pham T.L.G., Stuppner H., Ganzera M., Phytochemical study of *Rourea minor* stems and the analysis of therein contained Bergenin and Catechin derivatives by capillary electrophoresis, *Microchemical Journal*, 2019, **149**:104063 [Crossref], [Google Scholar], [Publisher]

[7]. Sase T.J., Bioltif Y.E., Ayika P., Gorip W.H., Dawulung J., Medicinal Potentials of Extracts of Nanoparticles Synthesized from the Stem Bark and Roots of *Rourea Minor* (*Santaloides afzelii*), *SSR Inst. Int. J. Life Sci*, 2020, **6**:2557 [Crossref], [Google Scholar], [Publisher]

[8]. Bischoff H., The mechanism of alpha-glucosidase inhibition in the management of diabetes, *Clinical and investigative medicine. Medecine clinique et experimentale*, 1995, **18**:303 [Google Scholar], [Publisher]

[9]. Deutschländer M.S., Van de Venter M., Roux S., Louw J., Lall N., Hypoglycaemic activity of four plant extracts traditionally used in South Africa for diabetes, *Journal of Ethnopharmacology,* 2009, **124**:619 [Crossref], [Google Scholar], [Publisher]

[10]. Gomathi D., Kalaiselvi M., Uma C., In vitro α-amylase and α-glucosidase inhibitory effects of ethanolic extract of *Evolvulus alsinoides* (L.), *International Research Journal of Pharmacy*, 2012, **3**:226 [Crossref], [Google Scholar]

[11]. Ademiluyi A.O., Oboh G., Soybean phenolic-rich extracts inhibit key enzymes linked to type 2 diabetes (α-amylase and α-glucosidase) and hypertension (angiotensin I converting enzyme) in vitro, *Experimental and toxicologic pathology*, 2013, **65**:305 [Crossref], [Google Scholar], [Publisher]

[12]. Hosseinimehr S.J., Azadbakht M., Abadi A.J., Protective effect of hawthorn extract against genotoxicity induced by cyclophosphamide in mouse bone marrow cells, *Environmental*

Toxicology and Pharmacology, 2008, **25**:51 [Crossref], [Google Scholar], [Publisher]
[13]. Wu L.L., Yang X.B., Huang Z.M., Liu H.Z., Wu G.X., In-vivo and in-vitro antiviral activity of hyperoside extracted from *Abelmoschus Manihot* (L) medik, *Acta Pharmacologica Sinica*, 2007, **28**:404 [Crossref], [Google Scholar], [Publisher]
[14]. Zhou T., Chen B., Fan G., Chai Y., Wu Y., Application of high-speed counter-current chromatography coupled with high-performance liquid chromatography diode array detection for the preparative isolation and purification of hyperoside from Hypericum perforatum with online purity monitoring, *Journal of Chromatography A*, 2006, **1116**:97 [Crossref], [Google Scholar], [Publisher]
[15]. Jirovetz L., Bail S., Buchbauer G., Denkova Z., Slavchev A., Stoyanova A., Schmidt E., Geissler M., Antimicrobial testings, gas chromatographic analysis and factory evaluation of essential oil of hop cones (*Humulus lupulus* L.) from Bavaria and some of its main compounds, *Scientia pharmaceutica*, 2006, **74**:189 [Crossref], [Google Scholar], [Publisher]
[16]. Li L., Yuge G., Jing W., Huirong Z., Xiaofei Z., Chun M.L., Preparative separation of hyperoside of seeds extracts of *Saposhnikovia divaricata* by high-performance counter-current chromatography, *Journal of Medicinal Plants Research*, 2012, **6**:884 [Crossref], [Google Scholar], [Publisher]
[17]. Raza A., Xu X., Sun H., Tang J., Ouyang Z., Pharmacological activities and pharmacokinetic study of hyperoside: A short review, *Tropical Journal of Pharmaceutical Research,* 2017, **16**:483 [Crossref], [Google Scholar], [Publisher]
[18]. Khandelwal K.R., Vrunda S. Extractive values. *Practical Pharmacognosy*; Nirali Prakashan: 19 thedn.; Budhwar Peth, India, 1975, p 157 [Publisher]
[19]. John B.I., Sulaiman C.T., George S., Reddy V.R., Total phenolics and flavonoids in selected medicinal plants from Kerala, *International Journal of Pharmacy and Pharmaceutical Sciences,* 2014, **6**:406 [Crossref], [Google Scholar], [Publisher]
[20]. Kyriakou E., Primikyri A., Charisiadis P., Katsoura M., Gerothanassis I.P, Stamatis H., Tzakos A.G., Unexpected Enzyme-Catalyzed Regioselective Acylation of Flavonoid Aglycones and rapid product screening, *Organic & biomolecular chemistry,* 2012, **10**:1739 [Crossref], [Google Scholar], [Publisher]
[21]. Chelladurai G.R.M., Chinnachamy. Alpha-amylasese and alpha-glucosidase inhibitory effects of aqueous stem extract of *Salacia oblonga* and its GC-MS analysis*, Brazilian Journal of Pharmaceutical Sciences*, 2018, **54**:e17151 [Crossref], [Google Scholar], [Publisher]
[22]. Mosmann T., Rapid Colorimetric Assay for Cellular Growth and Survival: Application to Proliferation and Cytotoxicity Assays, *Journal of immunological methods*, 1983, **65**:55 [Google Scholar]
[23]. Sagbo I.J., Van de Venter M., Koekemoer T., Bradley G., In vitro antidiabetic activity and mechanism of action of *Brachylaena elliptica* (Thunb.) DC, *Evidence-Based Complementary and Alternative Medicine,* 2018, **2018**:4170372 [Crossref], [Google Scholar], [Publisher]
[24]. Oshiomame Unuofin J., Aderonke Otunola G., Jide Afolayan A., In vitro a-amylase, a-glucosidase, lipase inhibitory, and cytotoxic activities of tuber extracts of *Kedrostis Africana* (L.) Cogn. *Heliyon*, 2018, **4**:e00810 [Crossref], [Google Scholar], [Publisher]
[25]. Apostolidis E., Kwon Y.I, Shetty K., Inhibitory potential of herb, fruit, and fungal-enriched cheese against key enzymes linked to type 2 diabetes and hypertension, *Innovative Food Science & Emerging Technologies*, 2017, **8**:46 [Crossref], [Google Scholar], [Publisher]
[26]. Al-Masri I.M., Mohammad M.K., Tahaa M.O. Inhibition of dipeptidyl peptidase IV (DPP IV) is one of the mechanisms explaining the hypoglycemic effect of berberine, *Journal of enzyme inhibition and medicinal chemistry*, 2009, **24**:1061 [Crossref], [Google Scholar], [Publisher]
[27]. Dąbrowska A.M., Tarach J.S., Kurowska M., 1,5-Anhydroglucitol (1,5-AG) and its usefulness in clinical practice, *Med. Biol. Sci*, 2012, **26**:11 [Crossref], [Google Scholar]
[28]. Aparna V., Dileep K.V., Mandal P.K., Karthe P., Sadasivan C., Haridas M., Anti-Inflammatory Property of n-Hexadecanoic Acid: Structural Evidence and Kinetic Assessment, *Chemical*

biology & drug design, 2012, **80**:434 [Crossref], [Google Scholar], [Publisher]
[29]. Ezekwe S.A., Chikezie P.C., GC-MS Analysis, Hypoglycemic Activity of Aqueous Root Extract of *Carica papaya* and Its Effects on Blood Lipid Profile and Hepatorenal Tissues Biomarkers of Diabetic Rats, *Journal of Diabetes and Metabolism*, 2017, **8**:740 [Crossref], [Google Scholar], [Publisher]
[30]. Silva R.O., Sousa F.B., Damasceno S.R., Carvalho N.S, Silva V.G., Oliveira F.R.M., Sousa D.P., Aragao K.S., Barbosa A.L., Freitas R.M., Medeiros J.V.R., Phytol, a diterpene alcohol, inhibits the inflammatory response by reducing cytokine production and oxidative stress, *Fundamental & Clinical Pharmacology,* 2014, **28**:455 [Crossref], [Google Scholar], [Publisher]
[31]. Elmazar M.M., El-Abhar H.S., Schaalan M.F., Farag N.A., Phytol/Phytanic Acid and Insulin Resistance: Potential Role of Phytanic Acid Proven by Docking Simulation and Modulation of Biochemical Alterations, *PLoS ONE*, 2013, **8**:e45638 [Crossref], [Google Scholar], [Publisher]
[32]. Fontana Pereira D., Cazarolli L.H., Lavado C., Mengatto V., Figueiredo M.S.R.B., Guedes A., Pizzolatti M.G., Silva F.R.M.B., Effects of flavonoids on α-glucosidase activity: Potential targets for glucose homeostasis, *Nutrition*, 2011, **27**:1161 [Crossref], [Google Scholar], [Publisher]
[33]. Adisakwattana S., Ruengsamran T., Kampa P., Sompong W., In vitro inhibitory effects of plant-based foods and their combinations on intestinal α-glucosidase and pancreatic α-amylase, *BMC complementary and alternative medicine*, 2012, **12**:1 [Crossref], [Google Scholar], [Publisher]
[34]. Kam A., Li K.M., Razmovski-Naumovski V., Nammi S., Shi J., Chan K., Li G.Q., A comparative study on the inhibitory effects of different parts and chemical constituents of pomegranate on α-amylase and α-glucosidase, *Phytotherapy Research*, 2013, **27:**1614 [Crossref], [Google Scholar], [Publisher]
[35]. Chowdhury S.S., Islam M.N., Jung H.A., Choi J.S., In vitro anti-diabetic potential of the fruits of *Crataegus pinnatifida*, *Research in pharmaceutical sciences,* 2014, **9**:11 [Google Scholar], [Publisher]
[36]. Verma N., Amresh G., Sahu P.K., Mishra N., Rao C.V, Singh A.P., Pharmacological evaluation of hyperin for antihyperglycemic activity and effect on lipid profile in diabetic rats, *Indian J. Exp. Biol*, 2013, **51**:65 [Google Scholar]

HOW TO CITE THIS ARTICLE
Ayat Monther Alqudsi, Khulood Abed Saleh, Isolation and Characterization of Hyperoside-flavanoidal Glycoside from *Rourea Minor* for its Anti-Hyperglycemic Activity Potential: An *in Vitro* Study. *J. Med. Chem. Sci*., 2023, 6(8) 1746-1762
https://doi.org/10.26655/JMCHEMSCI.2023.8.4
URL: http://www.jmchemsci.com/article_163472.html